

## Dynamics of two-magnon resonances in the absence of bound states

A. A. Baharmuz and P. D. Loly

*Department of Physics, University of Manitoba, Winnipeg, Manitoba, Canada, R3T 2N2*

(Received 13 March 1979)

Spectral intensity distributions are calculated for different types of spin-pair excitations in a simple-cubic Heisenberg ferromagnet with next-nearest-neighbor (nnn) exchange interactions. The ratio of next-nearest- to nearest-neighbor (nn) exchange interaction ( $\eta$ ) is chosen to be large enough to prevent the formation of bound states, by containing all pair excitations in the continuum, but without being too far removed from the nn case. Calculations have been performed using  $\eta = \frac{1}{8}$  and  $S = 1$  for single-ion, nn and nnn pair excitations for total pair wave vectors ( $\vec{K}$ ) along the [111] direction. An understandable picture of the excitations follows the study of resonance peaks in the computed spectra and their comparison with those of the nn case. The changes due to the relaxation of the exact Ising-like limit of the nearest-neighbor case at the zone boundary in the [111] direction are largely due to states which were formerly bound states having become resonances for all values of  $\vec{K}$ .

### I. INTRODUCTION

Most of the information on two-magnon pairing effects in ferromagnets has been obtained for the nearest-neighbor (nn) simple-cubic (sc) Heisenberg ferromagnet. In the isotropic case Wortis<sup>1</sup> and Hanus<sup>2</sup> demonstrated the presence of bound states outside the two-magnon continuum, Boyd and Callaway<sup>3</sup> showed that the doublet bound state broadened into a resonance inside the continuum, while Silberglitt and Harris<sup>4</sup> examined the effect of two-magnon resonances on the one-magnon propagator at finite temperatures. Various extensions have been made by other workers, especially for the incorporation of uniaxial anisotropy<sup>5,6</sup> and of biquadratic exchange.<sup>7,8</sup> The nn sc case possesses the special property of transforming to the associated Ising problem when the two magnons have a total wave vector ( $\vec{K}$ ) reaching the zone corner, as pointed out first by Wortis.<sup>1</sup> Loly and Choudhury<sup>9</sup> recently exploited this property to study the evolution of continuum resonances at  $\vec{K} = 0$  (the Raman mode) to bound states at the zone corner. This transition (from Heisenberg to Ising) follows a continuous shrinkage of the two-magnon (continuum) bandwidth as  $\vec{K}$  increases in the [111] direction until the limit is reached with zero bandwidth at the zone corner. A similar behavior occurs for the nn bcc case for  $\vec{K}$  along the [100] direction, where bound states have been shown to exist outside the continuum by Bonnot and Hanus<sup>10</sup> and by Saenz and Zachary.<sup>11</sup> These special features are not representative of the general case where there is a nonzero minimum bandwidth and therefore no corresponding Ising (discrete) limit. The fcc ferromagnet is a good example of a two-magnon continuum with nonzero minimum bandwidth (even in its nn case), while next-nearest-neighbor (nnn) interac-

tions have the same effect in the sc and bcc cases.

In the present work we are interested in understanding the factors that determine the position (frequency) of continuum resonances (of significance to Raman scattering experiments<sup>12</sup>) when they have no evolution in  $\vec{K}$  space to discrete Ising levels at the zone boundary. Correlations between Raman peaks and Ising levels have been noted in several instances [e.g., RbMnF<sub>3</sub> (Ref. 13) and mixed crystals (Ref. 14)] but it is not known if this is always to be expected. In this connection a thorough study of the nn sc case showed that an internal saddle-point singularity of the continuum gave a severe constraint to an important two-magnon resonance<sup>15</sup> and we suspect that the more complex singularity structure of the general case may play an important role in the determination of resonance frequencies.

In the course of a recent study of nnn interactions on the unperturbed two-magnon continuum of the sc ferromagnet<sup>16</sup> the present authors concluded that it would be instructive to do a fully interacting study of two-magnon effects in a case that was close to the nn limit of the well-understood sc case but without its pathological shrinkage and also avoiding any accidental critical-point degeneracies [e.g., for ratios of nnn to nn interaction ( $\eta = J_2/J_1$ ) equal to  $\frac{1}{4}$  (Ref. 16)]. The value of  $\eta$  equal to  $\frac{1}{8}$  appears to satisfy these requirements and is the case analyzed in the present paper. It should become clear below as we describe the analysis that the computational effort required for a single value of  $\eta$  is a severe deterrent to the extension of the present study to the other qualitatively distinct ranges of  $\eta$  surveyed recently by the authors.<sup>16</sup>

A spin Green's-function formalism<sup>17</sup> is ideally suited to the study of two-spin excitations in ferromagnets at absolute zero temperature because the equa-

tion of motion for the two-spin propagator terminates without the need for any decoupling approximations, thereby yielding an exact set of simultaneous equations for the Green functions of interest which is tractable if the range of exchange interactions is finite. We follow closely the formulation of Wortis<sup>1</sup> whose rigorous bound-state analysis for the ferromagnet predated intense interest in Raman scattering from transparent antiferromagnets, which was later put on a firm foundation by Elliot and Thorpe<sup>13</sup> using a similar spin Green's-function method. More recently Thorpe<sup>18</sup> renewed interest in two-magnon spectra in ferromagnets through a simplified spin Green's-function approach to Raman cross sections, since extended in several directions.<sup>7-9</sup>

Section II gives a compact outline of the development of the central equation for studying the complete  $\vec{K}$  dependence of the two-spin propagators at  $T = 0$  K for a Heisenberg ferromagnet with Ising-like anisotropy of arbitrary range and single-ion anisotropy. In application to the nnn sc case there are now a larger number of potentially interesting spectral probes than in the nn case and the matrix equations for their solutions are discussed in Sec. III. In Sec. IV the results of extensive numerical computations are summarized and the conclusions to be drawn from this study are given in Sec. V.

## II. TWO-MAGNON PROPAGATOR

In this section the two-magnon propagator is defined and an exact equation for it derived at absolute zero. This is then used, in Sec. III, to obtain the spectral functions for various two-spin excitation processes for the nnn sc ferromagnet. The Hamil-

tonian we consider is the Heisenberg Hamiltonian generalized to include both Ising and single-ion anisotropies

$$H = - \sum_{ij} (I_{ij} S_i^z S_j^z + J_{ij} S_i^+ S_j^-) - \sum_i D (S_i^z)^2, \quad (1)$$

where  $i$  is a shorthand notation for the position vector  $\vec{R}_i$ ,  $I_{ij}$  and  $J_{ij}$  are the longitudinal (Ising) and transverse exchange constants, respectively, between sites  $i$  and  $j$ , and  $D$  is the single-ion anisotropy. The propagator for the scattering of two magnons with initial wave vectors  $\vec{k}_1, \vec{k}_2$  and final wave vectors  $\vec{k}_1', \vec{k}_2'$  is

$$\begin{aligned} G(\vec{k}_1, \vec{k}_2, \vec{k}_1', \vec{k}_2', t) \\ = -i \Theta(t) \langle 0 | [S_{\vec{k}_1}^-(t) S_{\vec{k}_2}^-(t), S_{\vec{k}_1}^+(0) S_{\vec{k}_2}^+(0)] | 0 \rangle \\ = \langle \langle S_{\vec{k}_1}^-(t) S_{\vec{k}_2}^-(t) | S_{\vec{k}_1}^+(0) S_{\vec{k}_2}^+(0) \rangle \rangle, \quad (2) \end{aligned}$$

where  $S_{\vec{k}}^\alpha$  is the Fourier transform of  $S_i^\alpha$  and  $|0\rangle$  is the fully aligned ground state defined such that  $S^z|0\rangle = -S|0\rangle$  and  $S^\pm|0\rangle = 0$ . The equation of motion for the Green's function in Eq. (2) has the standard form

$$\begin{aligned} \omega G(\vec{k}_1, \vec{k}_2, \vec{k}_1', \vec{k}_2', \omega) \\ = \langle 0 | [S_{\vec{k}_1}^- S_{\vec{k}_2}^-, S_{\vec{k}_1}^+, S_{\vec{k}_2}^+] | 0 \rangle \\ + \langle \langle [S_{\vec{k}_1}^-(t) S_{\vec{k}_2}^-(t), H] | S_{\vec{k}_1}^+(0) S_{\vec{k}_2}^+(0) \rangle \rangle_\omega, \quad (3) \end{aligned}$$

where  $G(\dots, \omega)$  and  $\langle \langle \dots \rangle \rangle_\omega$  represent Fourier transforms. Evaluating the commutators in Eq. (3) gives

$$\begin{aligned} \{\omega - 2S[2I(0) - J(\frac{1}{2}\vec{K} + \vec{k}) - J(\frac{1}{2}\vec{K} - \vec{k})] - 2(2S - 1)D\} G(\vec{K}\vec{k}, \vec{K}'\vec{k}', \omega) \\ = 4S^2 \delta_{\vec{K}-\vec{K}'} \left[ \delta_{\vec{k}+\vec{k}'} + \delta_{\vec{k}-\vec{k}'} - \frac{1}{NS} \right] - \frac{2}{N} \sum_{\vec{q}} [I(\vec{q}) - J(\frac{1}{2}\vec{K} - \vec{k} - \vec{q}) + D] G(\vec{K}\vec{k} + \vec{q}, \vec{K}'\vec{k}', \omega), \quad (4) \end{aligned}$$

where we have made a change of variables to total and relative wave vectors defined as

$$\begin{aligned} \vec{K} = \vec{k}_1 + \vec{k}_2, \quad 2\vec{k} = \vec{k}_1 - \vec{k}_2, \\ \vec{K}' = \vec{k}_1' + \vec{k}_2', \quad 2\vec{k}' = \vec{k}_1' - \vec{k}_2'. \quad (5) \end{aligned}$$

In Eq. (4),  $I(\vec{q})$  and  $J(\vec{q})$  are the Fourier transforms of the longitudinal and transverse part of

the exchange interaction and  $N$  is the number of spins. Taking  $\vec{K} = \vec{K}'$  (conservation of total momentum) and introducing the partial Fourier transform

$$G(ij, \vec{K}, \omega) = \frac{1}{N} \sum_{\vec{k}, \vec{k}'} e^{-i\vec{k}\cdot\vec{R}_i} e^{i\vec{k}'\cdot\vec{R}_j} G(\vec{K}\vec{k}, \vec{K}'\vec{k}', \omega), \quad (6)$$

Eq. (4) reduces to

$$\begin{aligned} G(ij, \vec{K}, \omega) = 8S^2 \left[ 1 - \frac{\delta_{j0}}{2S} \right] \Lambda(ij, \vec{K}, \omega) + 2 \sum_l I_l \tilde{\Lambda}(il, \vec{K}, \omega) G(lj, \vec{K}, \omega) \\ + 2 \sum_l (J_l - I_l) [\Lambda(il, \vec{K}, \omega) + \tilde{\Lambda}(il, \vec{K}, \omega)] G(lj, \vec{K}, \omega) - 2 \sum_l D \Lambda(il, \vec{K}, \omega) G(lj, \vec{K}, \omega) \delta_{l0}, \quad (7) \end{aligned}$$

where

$$\Lambda(ij, \vec{K}, \omega) = \frac{1}{N} \sum_{\vec{k}} \frac{\cos \vec{k} \cdot \vec{R}_i \cos \vec{k} \cdot \vec{R}_j}{\omega - \Omega(\vec{K}, \vec{k})}, \quad (8)$$

$$\tilde{\Lambda}(ij, \vec{K}, \omega) = \frac{1}{N} \sum_{\vec{k}} \frac{\cos \vec{k} \cdot \vec{R}_i (\cos \frac{1}{2} \vec{K} \cdot \vec{R}_j - \cos \vec{k} \cdot \vec{R}_j)}{\omega - \Omega(\vec{K}, \vec{k})}, \quad (9)$$

and  $\Omega(\vec{K}, \vec{k})$  is the total energy of two noninteracting magnons given by

$$\Omega(\vec{K}, \vec{k}) = 2S[2J(0) - J(\frac{1}{2} \vec{K} + \vec{k}) - J(\frac{1}{2} \vec{K} - \vec{k})] + 2(2S - 1)D. \quad (10)$$

Equation (7) is the required equation for the two-magnon propagator.

### III. TWO-MAGNON SPECTRA

The spectral function for processes involving the creation of two spin deviations separated by a distance  $\vec{R}_i$  is given by the imaginary part of  $G(ii, \vec{K}, \omega)$ . Below we examine processes where two-spin deviations are created on the same site ( $\vec{R}_0 = (0, 0, 0)$ ), first-neighbor sites ( $\vec{R}_1 = (1, 0, 0)a$ ) and second-neighbor sites ( $\vec{R}_2 = (1, 1, 0)a$  or  $\vec{R}_2' = (1, -1, 0)a$ ) where  $a$  is the lattice constant. In shorthand notation these sites are denoted by  $i=0, 1, 2$  and  $2'$  respectively. We note here that for  $\vec{K}=0$ , Thorpe<sup>18</sup> has shown that  $-\text{Im}G(00, 0, \omega)$  is proportional to the

$$\Omega(\vec{K}, \vec{k}) = 4SJ(0) \{1 - \alpha/3\} (\cos x + \cos y + \cos z) - (2\eta/3) [\alpha^2 (\cos x \cos y + \cos y \cos z + \cos z \cos x) + \beta^2 (\sin x \sin y + \sin y \sin z + \sin z \sin x)] \}, \quad (12)$$

with  $\alpha = \cos(\frac{1}{2} K_x a)$ ,  $\beta^2 = 1 - \alpha^2$ ,  $x = k_x a$  etc., and  $\eta = J_2/J_1$  where  $J_1$  and  $J_2$  are the nearest- and next-nearest-neighbor exchange constants, respectively. These LGF's are evaluated using the tetrahedral scheme.<sup>19</sup> In the limit of  $\alpha=0$  (the zone corner) where the spectrum collapsed in the nn sc case we now have a spectrum of the nn fcc type and the LGF's are then expressed in terms of elliptic integrals of complex moduli and evaluated using the arithmetic-geometric mean method.<sup>20</sup>

From Eq. (7), we find that the equations for the four Green's functions mentioned above involve 14 LGF's and can be written more compactly in terms of two matrix equations. The first of these connects  $G(00, \vec{K}, \omega)$  to three off-diagonal Green's functions  $G(10, \vec{K}, \omega)$ ,  $G(20, \vec{K}, \omega)$ , and  $G(2'0, \vec{K}, \omega)$  and can

cross section for two-magnon Raman scattering through the spin-orbit interaction in ferromagnets, while the best analogue of the exchange process responsible for the antiferromagnetic observations is given by  $-\text{Im}G(11, 0, \omega)$  (which was studied earlier for the nn sc case<sup>9</sup>) and  $-\text{Im}G(22, 0, \omega)$ . In the context of discrete two-magnon bound states, in those situations where they are present outside the continuum, the nn pairs were originally investigated by Wortis<sup>1</sup> and by Hanus<sup>2</sup> with the single-ion pairs included later by Silberglitt and Torrance<sup>5</sup> and by Tonegawa<sup>6</sup> as a function of the single-ion anisotropy  $D$ . Though the extra variable is not desirable in our present study, the single-ion spectrum exists for  $D=0$  and it is instructive to compare it with the other types of processes.

It is clear that Eq. (7) represents a set of coupled equations involving various Green's functions which, in general, is quite complex. In this paper we consider an isotropic ( $I=J$  and  $D=0$ ) nnn sc ferromagnet and take the total pair wave vector  $\vec{K}$  to be in the [111]-direction for the sake of comparison with the nn case. The coefficients  $\Lambda$  and  $\tilde{\Lambda}$  which appear in Eq. (7) can be expressed in terms of the so-called lattice Green's functions (LGF's) defined as

$$L_i(\vec{K}, \omega) = \frac{1}{N} \sum_{\vec{k}} \frac{e^{i\vec{k} \cdot \vec{R}_i}}{\omega - \Omega(\vec{K}, \vec{k})}, \quad (11)$$

where the two-magnon dispersion function is given by

be written

$$\underline{A} \begin{pmatrix} G(00, \vec{K}, \omega) \\ G(10, \vec{K}, \omega) \\ G(20, \vec{K}, \omega) \\ G(2'0, \vec{K}, \omega) \end{pmatrix} = \left(1 - \frac{1}{2S}\right) \begin{pmatrix} L_0(\vec{K}, \omega) \\ L_1(\vec{K}, \omega) \\ L_2(\vec{K}, \omega) \\ L_{2'}(\vec{K}, \omega) \end{pmatrix}, \quad (13)$$

where  $\underline{A}$  is a  $4 \times 4$  matrix whose elements are functions of the LGF's. Since  $G(00, \vec{K}, \omega)$  vanishes for  $S = \frac{1}{2}$  we shall be mainly concerned with the case of  $S=1$  which has the largest resonance effects for all the processes indicated above.

The second equation determines the other three diagonal spectra that interest us and involves the Green's functions  $G(ij, \vec{K}, \omega)$  with  $i$  and  $j$  taking one of the nine values  $(1, 0, 0)a$ ,  $(0, 1, 0)a$ ,  $(0, 0, 1)a$ ,

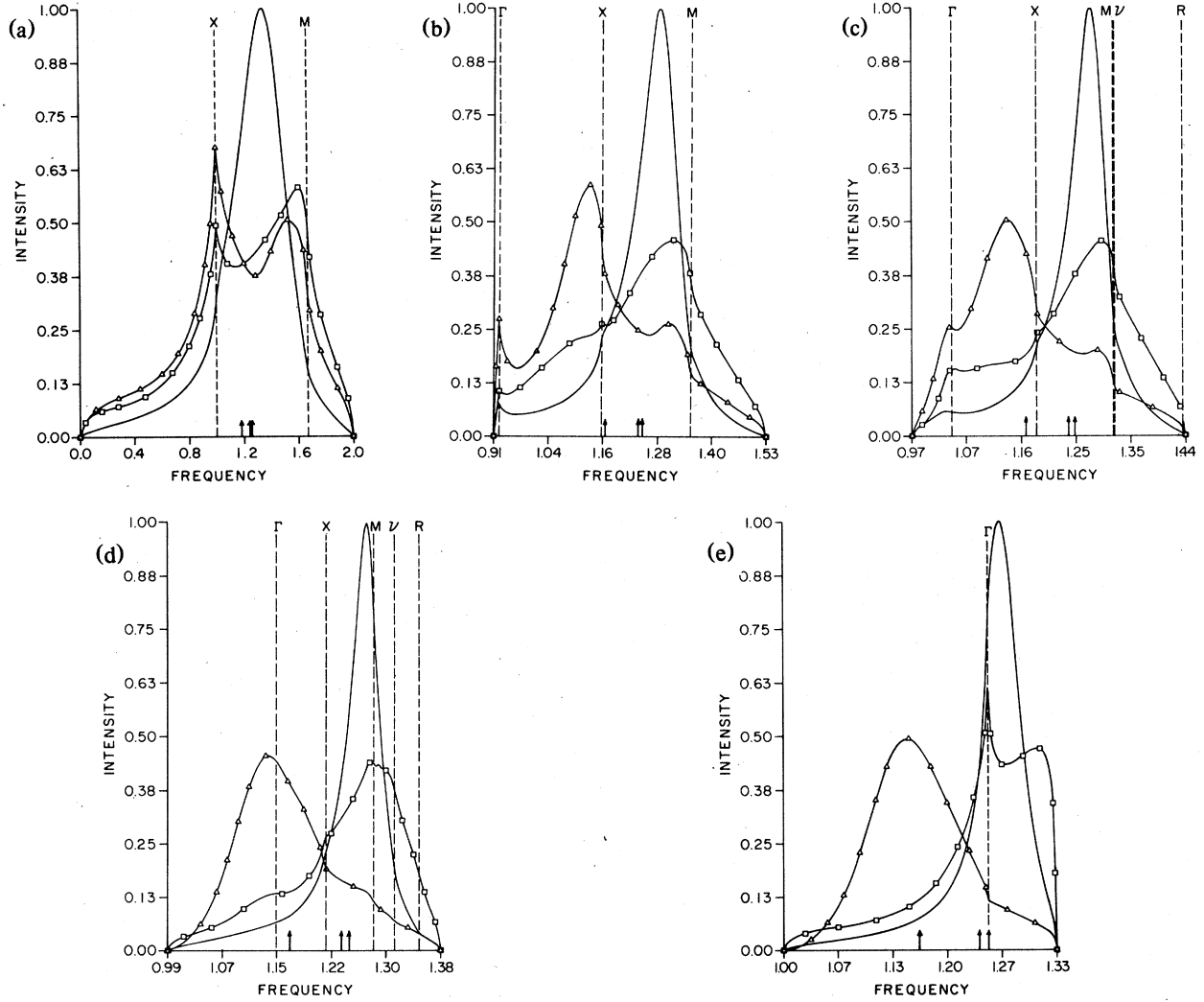


FIG. 1. Two-magnon spectra for the  $S=1$  nnn sc Heisenberg ferromagnet for representative values of the total pair wave vector  $\vec{K}$  in the  $[111]$  direction: (a)  $\alpha=1.0$ , (b)  $\alpha=0.3$ , (c)  $\alpha=0.2$ , (d)  $\alpha=0.1$ , and (e)  $\alpha=0.0$ , where  $\alpha=\cos(\frac{1}{2}K_x a)$ . The three curves represent 100 data points for the single-ion (solid line), nn (triangles) and nnn (squares) spectra. The three short arrows give the positions of nn, nnn, and single-ion Ising levels in that order from left to right while the vertical broken lines give the positions of critical points (see also Fig. 2).

$(1, 1, 0)a$ ,  $(0, 1, 1)a$ ,  $(1, 0, 1)a$ ,  $(1, -1, 0)a$ ,  
 $(0, 1, -1)a$ , and  $(-1, 1, 0)a$ . Denoting  $G(ij, \vec{K}, \omega)$  by  
the  $9 \times 9$  matrix  $\underline{G}(\vec{K}, \omega)$ , the second equation is  
written

$$\underline{B} \underline{G} = \underline{F}, \quad (14)$$

where  $\underline{B}$  and  $\underline{F}$  are  $9 \times 9$  matrices whose elements are functions of the LGF's. The dimension of 9 results from half (by inversion symmetry) of the total coordination number (nn plus nnn) though there are only 18 independent  $G$ 's.

#### IV. RESULTS

The main computational effort is associated with the evaluation and storage of the 14 LGF's for 11

values of  $\vec{K}$  and 100 frequency values for a single  $\eta$  value. After that, Eqs. (13) and (14) are solved by numerically inverting  $\underline{A}$  and  $\underline{B}$  and the spectral functions obtained for  $S=1$  and  $\eta=\frac{1}{8}$  are shown in Fig. 1 for several values of  $\vec{K}$ . For second neighbor excitations, the  $G(22, \vec{K}, \omega)$  and  $G(2'2', \vec{K}, \omega)$  spectra are very similar (they are exactly equal at the zone centre and corner) and we only present the results for the  $G(22, \vec{K}, \omega)$  spectrum here. The single-ion spectrum has only one resonance peak while the first and second neighbor ones each have an additional peak due to exchange resonances which behave similarly to the 'd-wave' of the nn case. All have indications of other structure that we shall discuss below.

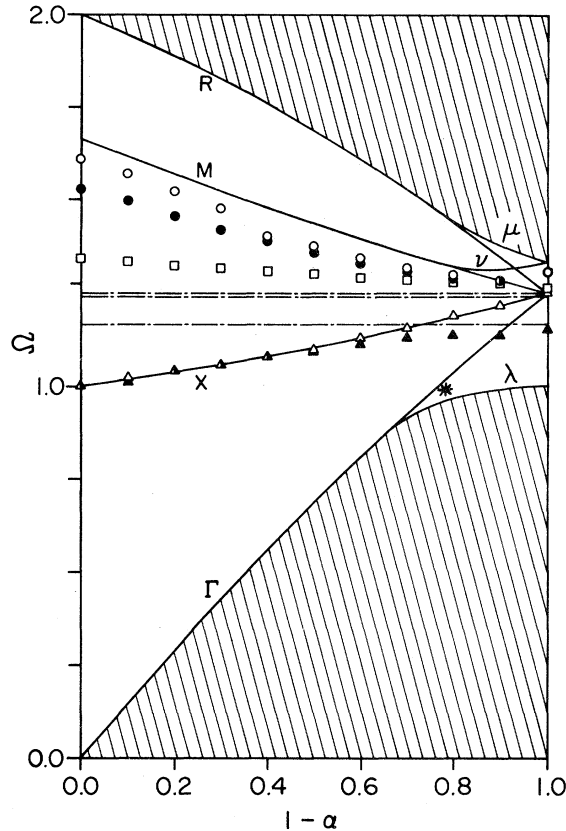


FIG. 2. Variation of the two-magnon resonance peak positions as a function of the total pair wave vector  $\bar{K}$  in the [111]-direction [ $\alpha = \cos(\frac{1}{2}K_x a)$ ]. The single-ion peaks in the  $G(00, \bar{K}, \omega)$ ,  $G(11, \bar{K}, \omega)$ , and  $G(22, \bar{K}, \omega)$  spectra are represented by open squares, solid circles and open circles respectively, while the dominant nn and nnn exchange resonance peaks in  $G(11, \bar{K}, \omega)$  and  $G(22, \bar{K}, \omega)$  are denoted by solid and open triangles, respectively. The unshaded region is the noninteracting two-magnon continuum, the full lines represent the critical points (Ref. 16) and the horizontal broken lines are the nn, nnn and single-ion Ising levels, respectively, in that order for increasing energy.

In addition, Fig. 1 shows a build-up of weight near the bottom of the band for values of  $\alpha$  between 0.2 and 0.4 and this may be recognized as the counterpart of the 's-wave' part of the nn exchange bound state which joined the continuum in a grazing fashion.

The positions of the main resonance peaks vary with  $\bar{K}$  as shown in Fig. 2 which has been constructed from plots for each spectrum taken at 11  $\bar{K}$  values from the zone center to its corner. For clarity the unshaded region represents the two-magnon continuum given by  $\Omega(\bar{K}, \bar{k})$  in Eq. (10) and the solid lines represent the two-magnon critical points found in the preceding paper.<sup>16</sup> The critical points are defined as points in  $\bar{k}$ -space where the group velocity ( $\nabla_{\bar{k}}\Omega(\bar{K}, \bar{k})$ ) for the two-magnon dispersion func-

tion vanishes. The critical points  $\Gamma$ ,  $X$ ,  $M$ , and  $R$  are the high symmetry points  $(0,0,0)$ ,  $(1,0,0)\pi/a$ ,  $(1,1,0)\pi/a$ , and  $(1,1,1)\pi/a$ , respectively, in the Brillouin zone. The other critical points  $\lambda$ ,  $\mu$ , and  $\nu$  move in  $\bar{k}$ -space as the pair wave vector varies. Also shown are the Ising levels for single-ion, first and second neighbor excitations. The Ising limit is obtained by neglecting the transverse terms in the exchange part of the Hamiltonian in Eq. (1). Thus the Ising levels for single-ion, first and second neighbor excitations are  $4SJ(0)$ ,  $4SJ(0) - J_1$ , and  $4SJ(0) - J_2$ , respectively.

The peak position of the single-ion spectrum  $G(00, \bar{K}, \omega)$ , shown in Fig. 2 decreases slowly as  $\bar{K}$  increases. The profiles also indicate a systematic narrowing of the main peak relative to the continuum bandwidth. This behavior is similar to the nn case except at the zone boundary where instead of the resonance peak coinciding with the Ising level for the creation of two spin deviations on a single site as in the nn problem, it is elevated somewhat having crossed the  $M$  and  $R$  singularities near the zone corner.

In contrast to the single-ion behavior, the other major peaks in the first and second neighbor spectra [ $G(11, \bar{K}, \omega)$  and  $G(22, \bar{K}, \omega)$ , respectively] disperse appreciably as  $\bar{K}$  varies. The exchange resonances are constrained (as in the nn case) below the  $X$  (saddle-point) singularity. For  $\alpha=0$  to 0.6, the lower peak in  $G(11, \bar{K}, \omega)$  occurs at a distinctly lower energy than for  $G(22, \bar{K}, \omega)$  and by comparison with the nn case we can be confident in identifying the former with the nn exchange resonance and the latter with the nnn one. For  $G(22, \bar{K}, \omega)$  there is a suggestion of the nn exchange resonance in the range  $\alpha=0.3$  to 0.1 as a structure on the lower energy side of the peak attributed to the nnn exchange resonance. We also see that a comparison between single-ion peaks in Fig. 2 reveals the effect of peak repulsions between the single-ion and 'd-wave' resonances, quite similar to the 'repulsion of energy levels' in atomic problems.

Turning to other structure in the spectra we identify the build up of weight near the bottom of the band in the range  $\alpha=0.2$  to 0.4 for all spectra as a result of the 's-wave' part of the nn exchange resonance being boxed in between the two merging critical points  $\Gamma$  and  $\lambda$  (denoted by an asterisk in Fig. 2). The separation of  $\Gamma$  and  $\lambda$  and the appearance of the nn 'd-wave' resonance between them as the zone corner is approached obscure the 's-wave' resonance in the range  $\alpha=0.2$  to 0.0.

## V. CONCLUSIONS

The type of analysis undertaken in this paper is costly in terms of computational (and plotting) effort because of the need to examine profiles at a large

number of  $\bar{K}$  values. However the general trends elucidated give a reasonable degree of confidence that the simpler analysis of the background (unperturbed) continuum structure as done for example in our preceding paper,<sup>16</sup> taken with a knowledge of the Ising levels, would enable one to predict the behavior of the resonances once a starting point (probably nn) has been established. This follows from the inability of either of the exchange resonances to penetrate the  $X$  saddle-point singularity, the absence of such a severe effect for the single-ion-type, together with the  $s$ -wave dispersion due to the  $\Gamma$  singularity.

Turning to the relaxation of the connection between resonance and bound-state positions to Ising levels which had followed in the nn case, we have found now that the resonances are generally shifted from the Ising levels at large values of  $\bar{K}$  (for both single-ion and exchange varieties). Since the formal transition to a discrete Ising problem is absent we should not be surprised. However, as long as the ratio of  $J_2/J_1$  is small, there should still be some correlation.

A similar departure of the bound-state energies from the Ising levels can be anticipated when such

states exist, in the nnn sc case for somewhat smaller values of  $\eta$  than  $\frac{1}{8}$ . The critical value of  $\eta$  for their existence is now not simply a matter of examining continuum edge and Ising levels with the result that  $\eta_c = 1/24S = 0.0416/S$  as thought initially.<sup>15</sup> Indeed Krompiewski<sup>21</sup> has recently given the critical value of  $J_2/J_1$  as 0.05 for  $S = 1$ , and one of us<sup>22</sup> (A.A.B.) has been able to obtain a definitive value of  $0.04645/S$  by noting that the bound-state condition at the zone corner ( $\alpha = 0$ ) obtained from our equations simplifies considerably and can be evaluated in terms of accurately attainable nn fcc lattice Green functions.<sup>20</sup>

In other cases it would still be interesting to have a full picture of the  $\bar{K}$  dependence of the behavior of resonances in the fcc ferromagnet where information available to date is for resonances at  $\bar{K} = 0$ ,<sup>23</sup> and bound states outside the continuum,<sup>24</sup> and also to follow the passage of the bound states of the nn bcc case as  $\bar{K}$  is decreased all the way through to  $\bar{K} = 0$ .<sup>10</sup>

#### ACKNOWLEDGMENT

This research was supported in part by the Natural Sciences and Engineering Research Council of Canada.

- <sup>1</sup>M. Wortis, Phys. Rev. **132**, 85 (1963).  
<sup>2</sup>J. Hanus, Phys. Rev. Lett. **11**, 336 (1963).  
<sup>3</sup>R. G. Boyd and J. Callaway, Phys. Rev. **138**, A1621 (1965).  
<sup>4</sup>R. Silbergliitt and A. B. Harris, Phys. Rev. Lett. **19**, 30 (1967); Phys. Rev. **174**, 640 (1968).  
<sup>5</sup>R. Silbergliitt and J. B. Torrance, Phys. Rev. B **2**, 772 (1970).  
<sup>6</sup>T. Tonegawa, Prog. Theor. Phys. Supp. **46**, 61 (1970).  
<sup>7</sup>D. A. Pink and P. Tremblay, Can. J. Phys. **50**, 1728 (1972); D. A. Pink and R. Ballard, Can. J. Phys. **52**, 33 (1974).  
<sup>8</sup>S. T. Chiu-Tsao, P. M. Levy, and C. Paulson, Phys. Rev. B **12**, 1819 (1975).  
<sup>9</sup>P. D. Loly and B. J. Choudhury, Phys. Rev. B **13**, 4019 (1976).  
<sup>10</sup>A. M. Bonnot and J. Hanus, Phys. Rev. B **7**, 2207 (1973).  
<sup>11</sup>A. W. Saenz and W. W. Zachary, J. Math. Phys. **14**, 1837 (1973).  
<sup>12</sup>R. J. Elliott, M. F. Thorpe, G. Imbusch, R. Loudon, and J. B. Parkinson, Phys. Rev. Lett. **21**, 147 (1968); R. J. Elliott and A. J. Smith, J. Phys. (Paris) **32**, C1-585 (1971).  
<sup>13</sup>R. J. Elliott and M. F. Thorpe, J. Phys. C **2**, 1630 (1969).  
<sup>14</sup>M. Buchanan, W. J. L. Buyers, R. J. Elliott, R. T. Harley, W. Hayes, A. M. Perry, and I. D. Saville, J. Phys. C **5**, 2011 (1972).  
<sup>15</sup>P. D. Loly, in *Proceedings of the Third International Conference on Light Scattering in Solids, Campinas, 1975*, edited by M. Balkanski (Flammarion, Paris, 1976), p. 274; P. D. Loly, in *Proceedings of NATO Advanced Study Institute on Correlation Functions and Quasiparticle Interactions, Minneapolis, 1977*, edited by J. Woods Halley (Plenum, New York, 1978), p. 319.  
<sup>16</sup>A. A. Baharmuz and P. D. Loly, Phys. Rev. B **19**, 5803 (1979).  
<sup>17</sup>See, for example, N. N. Bogolyubov and S. V. Tyablikov, Sov. Phys. Dokl. **4**, 604 (1959); D. N. Zubarev, Sov. Phys. Usp. **3**, 320 (1960); R. A. Tahir-Kheli and D. ter Haar, Phys. Rev. **127**, 88 (1962); M. Wortis, Ph.D. thesis (unpublished), and Ref. 1; J. F. Cooke and H. A. Gersch, Phys. Rev. **153**, 641 (1967); S. V. Tyablikov, *Methods in the Quantum Theory of Magnetism* (Plenum, New York, 1967); W. Marshall and G. Murray, J. Phys. C **2**, 539 (1969).  
<sup>18</sup>M. F. Thorpe, Phys. Rev. B **4**, 1608 (1971).  
<sup>19</sup>G. Lehmann and M. Taut, Phys. Status Solidi B **54**, 469 (1972).  
<sup>20</sup>M. Inoue, J. Math. Phys. **15**, 704 (1974); **16**, 111 (1975).  
<sup>21</sup>S. Krompiewski, Acta Phys. Pol. A53, 845 (1978).  
<sup>22</sup>A. A. Baharmuz (unpublished).  
<sup>23</sup>P. D. Loly, B. J. Choudhury, and W. R. Fehlner, Phys. Rev. B **11**, 1996 (1975); S. T. Chiu-Tsao, Phys. Rev. B **13**, 3175 (1976).  
<sup>24</sup>K. Wada and Y. Mizuta, Phys. Lett. A **59**, 311 (1976).